Available online at www.sciencedirect.com

SCIENCE DIRECT

Biochimica et Biophysica Acta 1707 (2005) 91–102

BIOCHIMICA ET BIOPHYSICA ACTA BBA

http://www.elsevier.com/locate/bba

Review

EPR techniques for studying radical enzymes

G. Jeschke*

Max Planck Institute for Polymer Research, Postfach 3148, Mainz D-55021, Germany

Received 17 July 2003; accepted 26 February 2004
Available online 18 May 2004

Abstract

EPR studies on radical enzymes are reviewed under the aspects of the information that they can provide and of the techniques that are used. An overview of organic radicals derived from amino acids, modified amino acids, and cofactors is given and *g* tensor data are compiled. The information accessible from a spectroscopic point of view is contrasted with the information required to understand enzyme structure and function, and some precautions are discussed that must be taken to derive the latter kind of information from the former. Structural dynamics is identified as an aspect that has rarely been addressed in the past although it is highly relevant for enzyme function. It is proposed that techniques introduced recently on other classes of proteins could help to close this gap.

Keywords: EPR; ENDOR; Tyrosyl radical; Glycyl radical; Ribonucleotide reductase; Cob(II)alamine

1. Introduction

Many enzymatically catalysed processes involve one-electron oxidation or reaction steps. For a diamagnetic resting state of the enzyme, which is the usual case, this implies a paramagnetic transient state that is, at least in principle, detectable by EPR spectroscopy. Often the unpaired electron is centred at a transition metal (metalloenzymes), but in a number of cases the paramagnetic centre is a radical derived from a native or post-translationally modified amino acid (radical enzymes in a strict sense) or from a cofactor (enzymes using a radical mechanism) [1–5]. Radical states may also be involved in suicide inactivation of enzymes [2]. To understand the function of such enzymes on a molecular level, it is necessary to detect and identify the paramagnetic centre, to localise it in the protein or protein–substrate complex, and to get information on the reaction steps involved in its formation and decay (including their kinetics). Finally, it may be desirable to elaborate details of electronic and geometric structure to obtain insight into how the protein controls its reactivity. Due to the complexity of the structure and dynamics of such systems, a research program like this requires the complementary use of different spectroscopies (EPR, NMR, Raman, UV/vis) and, in cases where the protein can be crystallised, of X-ray diffraction. For the radical state itself, EPR spectroscopy is usually the method that provides the most reliable and detailed information.

In this selective review, we illustrate how EPR spectroscopy has been used for this purpose and try to point out some opportunities that have not been utilised to date. In particular, we emphasise that modern EPR [6–10] offers a broad variety of experimental techniques. By choosing the experiment appropriate for the aspect of interest, complexity can be considerably reduced. The review is organised as follows. Section 2 provides an overview of organic radicals that have so far been identified to be part of an enzymatic process, excluding radicals that are specific to photosynthetic reaction centres, which have been reviewed recently [8,10,11], and radicals derived from substrates. Basic information on their structure and EPR properties is provided to set the stage for the following discussions. Section 3 considers the structural and dynamic information about a radical that is generally accessible from EPR experiments, while Section 4 attempts to relate this to the questions of interest in the context of enzymatic catalysis. Both Sections 3 and 4 address the choice of a technique to obtain the desired piece of information.

* Tel.: +49-6131-379-100; fax: +49-6131-379-126.
E-mail address: jeschke@mpip-mainz.mpg.de (G. Jeschke).

0005-2728/$ - see front matter © 2004 Elsevier B.V. All rights reserved.
doi:10.1016/j.bbabio.2004.02.012

2. Radicals in enzymes

2.1. Radicals derived from intrinsic amino acids

Hydrogen abstraction from the four native amino acids tyrosine, tryptophan, glycine, and cysteine results in formation of reasonably stable radical species, **1**, **2**, **3**, and **4**, respectively (Scheme 1). Note that mechanistic details of this process may differ for the different radical enzymes, with proton-coupled electron transfer being a viable alternative to simple transfer of a hydrogen atom [12]. As the time scale of both alternative processes is too fast for reliably distinguishing between them by existing EPR techniques, we restrict the following discussion to the product radicals which are the same. The tyrosyl radical **1**, which occurs in class I ribonucleotide reductase, prostaglandin H synthase, Photosystem II, and possibly in dopamine β monooxygenase [1,13], can be readily detected by EPR spectroscopy. The spectrum is characterised by an orthorhombic g tensor (Table 1), which can be resolved at high fields/frequencies [8,14–17], a resolved hyperfine coupling to one of the aliphatic β protons ($H_{\beta 1}$, see Fig. 1) [14], and unresolved hyperfine couplings to the other β proton and to the aromatic protons which were determined by high-field electron-nuclear double resonance (ENDOR) spectroscopy [18]. For reasons discussed in Section 3, the g_x value is rather sensitive to the protein environment [16] (see also Table 1).

Tryptophanyl radicals **2** are involved in enzymatic action of ribonucleotide reductase [19], DNA photolyase [20], and cytochrome c peroxidase [15]. The occurrence of a tryptophanyl radical at residue Trp171 of lignin peroxidase during oxidation of substrates by this enzyme has been proved by spin trapping [21] with methyl nitroso propane and subsequent crystal structure analysis of the spin trap adduct [22]. EPR studies on tryptophanyl radicals are still scarce. However, the recent determination of the g tensor [19] (see Table 1) may open up new opportunities for these proteins as this knowledge can aid data analysis in cases where the radical is weakly coupled to metal centres or other radicals [15].

Glycyl radicals **3** are unique in the sense that the radical centre is localised on the peptide main chain. They are unstable in the presence of oxygen and thus seem to be restricted to enzymatic processes under anaerobic conditions, as in pyruvate formate-lyases, anaerobic class III ribonucleotide reductases, and benzylsuccinate synthase [5,23]. Resolution of the g tensor (Table 1) requires high magnetic fields and has been achieved only very recently [24].

Thiyl radicals **4** have been postulated as intermediates of pyruvate formate-lyase [25] and of all three known classes of ribonucleotide reductase [1]. Due to the large spin-orbit

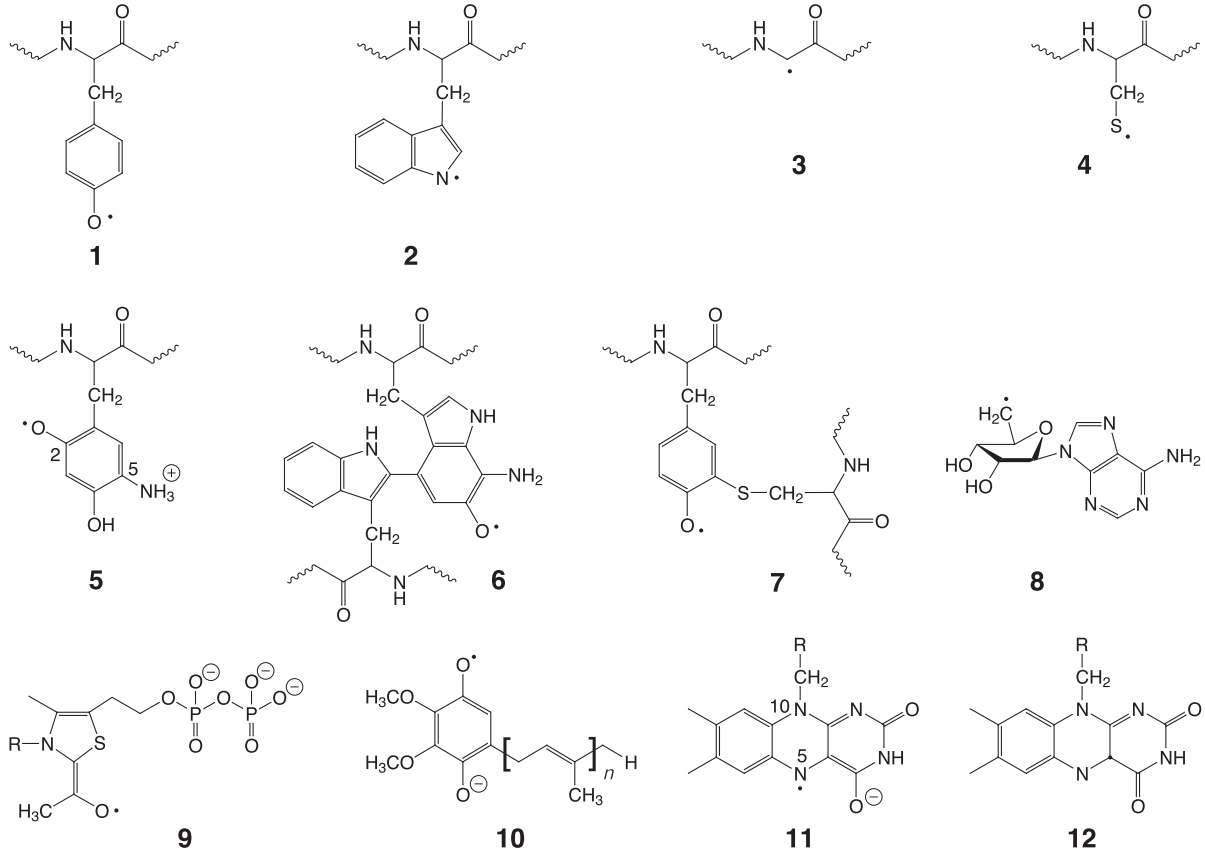

Scheme 1.

Table 1
Principal values of the g tensors of selected radicals involved in enzymatic catalysis

Radical	g_x	g_y	g_z	Remarks	References
1	2.0065–2.0091	2.0040–2.0043	2.0021	resolved proton hfi	[14–17,39]
2	2.0033–2.0035	2.0024–2.0025	2.0021		[15,19]
3	2.0042–2.0047	2.0031–2.0039	2.0020–2.0025	resolved hfi α proton	[23,24]
4	2.16–2.50	2.0080–2.0084	2.0080–2.0084	substantial g strain for g_z component	[26–29]
5	2.005	2.005	2.002	unresolved hfi	[33]
7	2.0074	2.0064	2.0021	weakly resolved hfi	[39]
10	2.0059	2.0054	2.0022		[48,50]
11	2.00436	2.00402	2.00228	nitrogen hfi	[53]
12	2.00425	2.00360	2.00227	nitrogen hfi	[54]

For structures, see Scheme 1; for further EPR parameters, see Ref. [1].

coupling constant of sulfur, electron spin relaxation is too fast for detection in solution, and due to near-degeneracy of orbitals, the g_x value is extremely sensitive to interactions with the matrix, in particular, to formation of hydrogen bonds that break axial symmetry about the C—S bond [26]. Indirect EPR detection at room temperature is possible by spin trapping with 5,5-dimethyl-1-pyrroline *N*-oxide [27] or phenyl-*N*-*t*-butylnitrone [28], while direct detection has been achieved after UV irradiation of *Escherichia coli* ribonucleotide reductase at 77 K [29,30]. Strong g strain along the direction of the C—S bond (x direction) renders the g_x feature unobservable for ribonucleotide reductase, while for bovine serine albumine such a feature could be observed ($g_x = 2.18$), presumably due to stronger hydrogen bonding.

2.2. Radicals derived from modified amino acids

In some enzymes, such as amine oxidase, methylamine dehydrogenase, and galactose oxidase, radical centres are located at post-translationally modified amino acids [1,3]. In copper-dependent amine oxidase, radical **5** is derived from the topa quinone, which is a tyrosine residue dihydroxylated

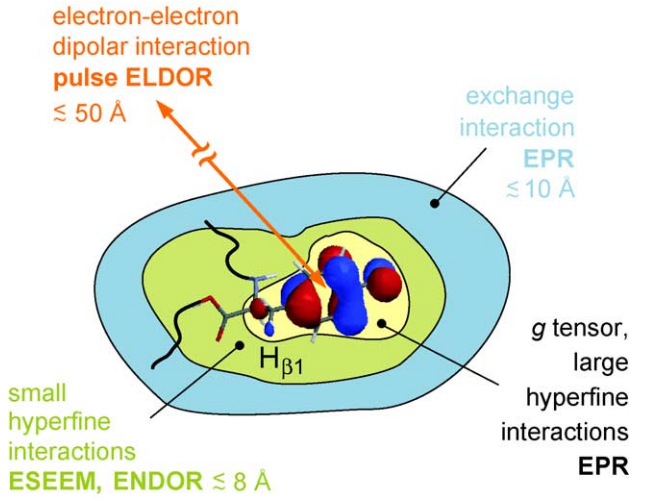

Fig. 1. SOMO of the tyrosyl radical and overview of interactions of the electron spin, of methods for their determination, and of the length scales they probe.

in the 2 and 5 positions and oxidated to the quinone. Radical **5** is formed by reaction of the keto group in 5-position with the substrate to an imine, subsequent hydrolysis of this imine, and transfer of one electron to a nearby type 2 Cu^{II} centre that yields Cu^{I} and the semiquinoid radical [31]. The presence of a substrate-derived nitrogen nucleus in this radical was detected by electron spin-echo envelope modulation (ESEEM) spectroscopy [32]. The best estimate to date for the g tensor of this radical (Table 1) has been obtained by Q-band EPR [33], however, resolution at this frequency is still poor and measurements at a significantly higher field may be necessary.

Radical **6** in methylamine dehydrogenase derives from tryptophan tryptophanyl quinone and is unusual in that it links two sections of the protein main chain (e.g. tryptophan quinone residue (Trq)55 and tryptophan residue Trp 106 in *Methylobacterium extorquens*). Residue (Trq)55 is a dihydroxylated tryptophan which has autooxidised to the ortho-quinone. The g tensor is unresolved at X-band, the assignment to the N-form rather than O-form of the semiquinone is based on an ESEEM study [34].

A linkage between two sections of the protein main chain (Tyr272 and Cys228) is also provided by the modified tyrosine radical **7** in galactose oxidase [35]. Although biogenesis of this cofactor requires the presence of copper ions [36], with Cu(I) being more effective than Cu(II) [37], the radical can be observed by EPR only in the chemically oxidised copper-free apoprotein, as it couples antiferromagnetically to the copper ion in the active enzyme [38]. The principal values of the g tensor of this radical (Table 1) are significantly different from those ones of unsubstituted tyrosyl radicals [39], and these differences have recently been well understood on the basis of density functional theory (DFT) computations [40]. Lysyl tyrosylquinone in lysyl oxidase [41] is another source for semiquinoid radicals derived from a modified amino acid. To the best of our knowledge, no EPR work has been published to date with respect to this putative radical.

2.3. Radicals derived from cofactors

Several enzymes, e.g. pyruvate formate-lyase, lysine 2,3-aminomutase, anaerobic ribonucleotide reductase, and bio-

tin synthase, use a one-electron transfer from a reduced iron–sulfur cluster to *S*-adenosylmethionine to produce the highly reactive 5′-deoxyadenosyl radical **8** [2]. Direct observation of this radical by EPR spectroscopy under conditions typical for enzymatic catalysis has not succeeded to date. However, using the sensitivity advantage of chemically induced dynamic electron polarization (CIDEP) after photoinduced homolytic bond cleavage of 5′-deoxyadenosyl-cobalamine, this short-lived radical could be observed [42]. The isotropic g value is 2.0097, the hyperfine splitting due to the α protons is 2.21 mT, and two further doublet splittings of 0.161 and 0.059 mT were assigned to the neighbouring protons in the five-membered ring.

Pyruvate:ferredoxine oxidoreductase effects the oxidative decarboxylation of pyruvate by a mechanism that depends on the thiamine pyrophosphate (TPP) group and two [Fe_4S_4] clusters as cofactors. On reaction of the enzyme with pyruvate an EPR line centred at $g=2.008$ is observed. This line has been assigned to radical **9** in which the acetyl group derives from the substrate, as was demonstrated by substitution of the three protons of the methyl group (carbon 3) of pyruvate by deuterons [43]. An ENDOR study provided the proton hyperfine couplings and revealed a ^{31}P hyperfine coupling of approximately 0.4 MHz [44]. The latter results could be modelled with a σ-type radical with few spin density distributed over the thiamine moiety or, alternatively, by a π-type radical with a methyl group that is rapidly rotating at a temperature of 4 K. A recent crystal structure of the free radical intermediate shows that the thiamine moiety is not planar and thus suggests a slightly different electronic structure than **9** [45]. Measuring the principal values of the g tensor by high-field EPR and comparing them to DFT computations would probably definitively clarify the electronic structure.

Quinones are nearly ubiquitous cofactors in redox-active enzymes [46], and consequently a whole book had been devoted to their EPR spectra as early as 1985 [47]. One-electron reduction of quinones leads to semiquinone radicals, for which the anion radical **10** derived from ubiquinone in quinol oxidase is an example [48]. The g tensor of such semiquinone radicals is partially resolved at Q-band frequencies of about 35 GHz [49] and almost completely resolved at W-band frequencies of about 95 GHz [50]. Principal values of the g tensor are sensitive to the type of quinone (substituents) and to hydrogen bonding [49,51]. Recent DFT computations reproduce experimental results quite well and provide a good overview of these dependencies [52].

Flavin semiquinones, such as anion radical **11** observed in Na^+-translocating NADH:quinone oxidoreductase [53], can be readily distinguished from other semiquinones due to the substantial hyperfine couplings to the nitrogen nuclei N(5) and N(10) ($A_z=22.8$ MHz) normal to the plane of the aromatic system, which are $A_z=57.6$ and 22.8 MHz, respectively. Slightly different values are found for the neutral radical **12**. There are also slight but perceptible differences in the g tensor principal values of the anion radical (Table 1) and the neutral flavine radical [54].

3. The spectroscopist's view: what an electron spin can see

3.1. Electronic structure

The organic radicals considered in this review have one unpaired electron, i.e. total electron spin $S=1/2$. Three interactions of the electron spin with its environment are directly related to the *electronic* structure of the paramagnetic centre. These are the spin-orbit interaction that causes a shift of the g value with respect to the free electron value $g_e=2.002319$, which is usually anisotropic, the Fermi contact interaction with nuclei which causes isotropic hyperfine couplings, and the exchange interaction with the unpaired electrons of other paramagnetic centres. The exchange interaction is due to partial overlap of orbitals which causes anisotropic exchange coupling at short distances r between centres (less than 5 Å) and isotropic exchange coupling at larger distances r. The isotropic exchange coupling scales roughly with $\exp(-r)$.

The shifts in the g value are a *global* characteristic of the singly occupied molecular orbital (SOMO) and of the molecular orbitals of low-lying excited states. The importance of excited states derives from the fact that orbital momentum is quenched in a non-degenerate electronic ground state, so that the g shifts are usually related to an admixture of excited states [55]. As this admixture requires overlap of orbitals and the SOMO is always involved, the symmetry or pseudosymmetry of the g tensor is often a good indication for the symmetry of the SOMO. According to perturbation theory, the extent of the admixture and thus the magnitude of the g shifts increases with decreasing energy difference between the ground state and the excited states and with increasing spin-orbit coupling constant. As a rule of thumb, the spin-orbit coupling constant increases with the atomic number as spin-orbit coupling is a relativistic effect. For instance, this constant is 382 cm^{-1} for sulfur, but only 151 cm^{-1} for oxygen. Therefore, organic radicals, which consist of light elements, usually feature only small g shifts (less than 10^{-2}, see Table 1). Alkyl thiyl radicals such as the one derived from cysteine are an exception for two reasons. First, they have a first excited state that is nearly degenerate with the ground state, and second, spin-orbit coupling is larger for sulfur than for second-row elements.

The g shifts are also sensitive to the environment of the paramagnetic centre, since the presence of electric dipoles in polar solvents or the formation of hydrogen bonds influence the energy difference between the ground state and the first excited state [49,51,56]. Precise measurements of g shifts and comparison among different proteins [16], with model systems [39], or with DFT computations [52] may thus

provide information that goes beyond the fingerprint information of the g tensor for identifying the radical. Such precise measurements for organic radicals require at least Q-band frequencies (35 GHz) and in most cases even higher frequencies and fields (W-band, 95 GHz; D-band, 140 GHz). In a sizeable number of cases, complete resolution of the g tensor requires frequencies above 140 GHz. If g anisotropy does not clearly dominate the spectral line shape at the highest available fields and frequencies, multi-frequency EPR is required to separate the g tensor from other interactions. In this approach, the EPR spectrum is measured at several frequencies spread over at least one order of magnitude and the frequency dependence of the line shape is analysed.

The Fermi contact interaction of the electron spin with a nuclear spin is directly related to spin density in the s orbital of this nucleus, it thus provides information on the delocalisation of the SOMO. This is most conveniently probed by proton hyperfine couplings, which, mediated by a spin polarisation mechanism, reflect spin density on the atom to which the proton is bound. The anisotropic hyperfine coupling is more difficult to interpret, as it may contain contributions from spin density in p or d orbitals on the nucleus under consideration as well as a through-space contribution due to dipole–dipole coupling to electron spin density in other parts of the radical. The former contribution dominates if the spin is centred on this nucleus, the latter contribution usually dominates for spin densities of less than 1% at this nucleus. An analysis of the anisotropic hyperfine coupling therefore presupposes a full understanding of the electronic structure. Recent advances in computational chemistry [40,57,58] allow for such an understanding to be gained.

Hyperfine couplings are also influenced by the environment of the paramagnetic centre, but in contrast to the global sensitivity of the g tensor, they exhibit local sensitivity in the vicinity of the nucleus under consideration. This difference can be used to separate effects due to polarity of the environment from effects due to hydrogen bonding, as has recently been demonstrated for nitroxide spin labels in bacteriorhodopsin [59].

Hyperfine couplings larger than approximately 10 MHz or 0.4 mT are often resolved in EPR spectra. For measurements with higher precision or measurements of smaller hyperfine couplings, ENDOR techniques are usually best suited. Among them, CW ENDOR [60] is the method of choice for work in solution. For the investigation of freeze-quenched preparations at low temperature, pulse ENDOR methods [7] are often, though not always, more favourable. For the measurement of very small couplings, ESEEM techniques [7,61] can be advantageous. This applies in particular to nuclei with low gyromagnetic ratio, such as ^{14}N and ^{2}H, when the measurements are performed at EPR frequencies up to X-band. While high-field ENDOR (at Q-band and in particular, at W-band frequencies) appears to be even better for ^{2}H, ESEEM at X-band frequencies or at multiple frequencies up to Q-band is probably the best choice for weakly coupled ^{14}N nuclei. This is also due to the fact that two-dimensional techniques such as HYSCORE [62] and DONUT-HYSCORE [63] significantly aid peak assignment and increase the reliability of spectral analysis. Magnitude and asymmetry of the nuclear quadrupole coupling of a ^{14}N nucleus are related to the type of bonding and can often be used to distinguish between nitrogens in cofactors, amide nitrogens of the peptide bond, and additional nitrogen atoms in amino acids such as histidine or arginine.

Primary radicals in proteins are often located close to another paramagnetic centre as they are usually generated by one-electron transfer from a metal cofactor [1]. This transfer creates a second paramagnetic centre at the metal, except for the case of Cu(II) cofactors which are reduced to diamagnetic Cu(I) centres. In a non-conducting matrix, the wave functions of paramagnetic centres overlap significantly, i.e. exhibit observable exchange coupling, up to distances between the centres of at least 10 Å. If the matrix favours electron transfer, as may be expected for redox active enzymes, significant overlap may be observable at even larger distances. A particularly large antiferromagnetic exchange coupling of 0.72 cm^{-1} between an $[4Fe–4S]^{+}$ cluster and a flavine mononucleotide radical has been observed in trimethylamine dehydrogenase where the centre-to-centre distance according to the crystal structure is 10.6 Å, suggesting that exchange proceeds along a network of covalent bonds and hydrogen bonds rather than through space [64]. Large exchange couplings can be determined by line shape analysis of EPR spectra, in particular, when measurements at multiple frequencies have been performed [64]. Small exchange couplings between an organic radical centre and the much faster relaxing electron spin of a metal centre can be inferred from saturation-recovery relaxation measurements as a function of temperature [65,66]. In photosynthetic reaction centres from *Rh. sphaeroides*, an intermediate semiquinone biradical state $Q_A^{-}\cdot Q_B^{-}\cdot$ could be trapped and the dipole–dipole and exchange coupling between the constituent radicals could be determined by analysing spectra obtained at frequencies of 9.6, 35, and 94 GHz [67]. This analysis provided information on the relative position and orientation of the two radicals, which compared well with X-ray diffraction data for the $Q_AQ_B^{-}\cdot$ state.

3.2. Geometric structure

The electron spin of a paramagnetic centre and the nuclear spins surrounding it are magnetic dipoles. For the moment, we assume that the two spins are well localised on the length scale of the distance between them. This point–dipole approximation generally applies to nuclear spins, but may be violated for electron spins. Within the point–dipole approximation, the dipole–dipole interaction between a pair of spins with distance r is proportional to r^{-3}. The orientation dependence of this interaction is particularly simple when both spins are quantised along the external magnetic

field. This is true for electron spins with small g anisotropy (all organic radicals except, perhaps, alkyl thiyl radicals) and for the nuclear spins of atoms where few electron spin density is located. In this case, the orientation dependence of the dipole–dipole coupling is completely characterised by the second Legendre polynomial $(3\cos^2\theta - 1)/2$ of the angle θ between the external field and the spin–spin vector. By measuring the magnitude of the dipole–dipole interaction and its orientation dependence in a reference frame, it is thus possible to completely determine length and orientation of the spin–spin vector. If single crystals are available, a crystallographic frame related to the unit cell can be used as the reference frame, otherwise it may be possible to use the principal axis frame of the g tensor (molecular frame). The latter frame can in turn be related to the molecular geometry by symmetry considerations, considerations on the main contributions to the SOMO, or by quantum-chemical computations (for instance, DFT computations).

Complications in this procedure occur for measurements of the distance between the electron spin of an organic radical and a metal centre, when the metal centre has large g anisotropy. In this case, the electron spin of the metal centre is not necessarily quantised along the external field and the orientation dependence of the dipole–dipole coupling becomes more complicated [7]. A more intricate complication has been found recently for strongly coupled clusters of several metal ions [68]. In this case, the dipole–dipole coupling depends on the inner structure of the cluster, i.e. on the coupling scheme for the metal ions.

The procedure for determining the spin–spin vector also needs to be modified when the electron spin is significantly delocalised on the length scale of the spin–spin distance. In this situation, some model for the delocalisation of the electron spin has to be assumed, for instance, a model derived from a measurement of isotropic hyperfine couplings. Fractions of spin density can then be assigned to the atoms in the radical, the point–dipole approximation is applied to each atom separately, and the spin-density-weighted average of the coupling is computed [7]. Alternatively, the measured values for the dipole–dipole interaction can be compared to values from a quantum-chemical computation and can be used to refine the geometry assumed in this computation.

For electron-nuclear spin pairs, the dipolar part of the hyperfine coupling can be measured with ENDOR and ESEEM techniques as discussed above. In ESEEM spectra, the dipolar part of the coupling causes a shift of the sum combination frequency with respect to twice the nuclear Zeeman frequency [7]. This shift can be measured most precisely by four-pulse ESEEM spectroscopy [69,70]. The dipolar part also determines the modulation depth in ESEEM experiments, which is proportional to r^{-6} and to the number of contributing nuclei [7]. The decay of the modulation also depends on r and the number of nuclei, but in a different way, so that the two parameters can be separated [70,71].

The dipole–dipole coupling between electron spins can be determined from measurements of the intensity of the half-field transition ($r = 5–10$ Å), from line shape analysis in CW EPR spectra ($r = 10–20$ Å), and by several pulse EPR techniques ($r = 20–80$ Å) [66]. Measurements by pulse techniques and the corresponding data analysis have been discussed in detail recently [72].

3.3. Dynamics

EPR experiments can directly detect dynamic processes over a broad range of time scales from the picosecond to the millisecond range. Processes that have shorter correlation times τ_c than 1–10 ps cause complete isotropic averaging of the spectra (Fig. 2a) and do not significantly influence relaxation times. Processes with $\tau_c > 1$ ms cannot usually be detected as the electron spins lose memory on the time scale of their longitudinal relaxation time which may range from 100 ns to 1 ms for the species and temperature range of interest in this review. Kinetics can be followed on time scales from seconds to hours if the process of interest creates or destroys paramagnetic centres or changes their spectra. In this case the EPR spectrum is measured repeatedly and changes in radical concentration (double integral of the CW EPR spectra, integral of FT EPR or echo-detected EPR spectra) or in the line shape are analysed.

For 1 μs $< \tau_c <$ 1 ms, dynamics can be characterised by pulse EPR measurements [7] or by saturation transfer methods [73]. Simple and sensitive CW EPR measurements may provide a wealth of information on rotational diffusion when the correlation times correspond to the slow tumbling regime [74,75]. The upper limit of correlation times for this regime is set by the transverse relaxation time T_2. Slower motion does not affect the EPR line shape (Fig. 2c). Line broadening due to unresolved hyperfine interaction with a typical line width Γ can mask even faster dynamics down to correlation times $\tau_c \approx 1/\Gamma$. The lower correlation time limit for the slow tumbling regime depends on the total anisotropy $\Delta\nu$ (in MHz) of the EPR spectrum, which is usually well approximated by the total width of the spectrum (Fig. 2c). Slow tumbling extends down to correlation times of approximately $1/(10\Delta\nu)$. Faster motion is still relevant for transverse relaxation and can thus be studied by analysing line widths [76].

CW EPR spectra are most sensitive to the details of the rotational diffusion process for $\tau_c \approx 1/\Delta\nu$ (Fig. 2b). It is possible to infer from the line shapes whether reorientation dynamics is restricted or unrestricted. For unrestricted Brownian diffusion, it is possible to determine rotational diffusion tensors, in other words, to decide whether a molecule has a preferential axis of rotation (Fig. 2d). Restricted motion of nitroxide spin labels could be successfully simulated by deriving a potential from a molecular dynamics run and computing the EPR line shape for Brownian motion in this potential [77].

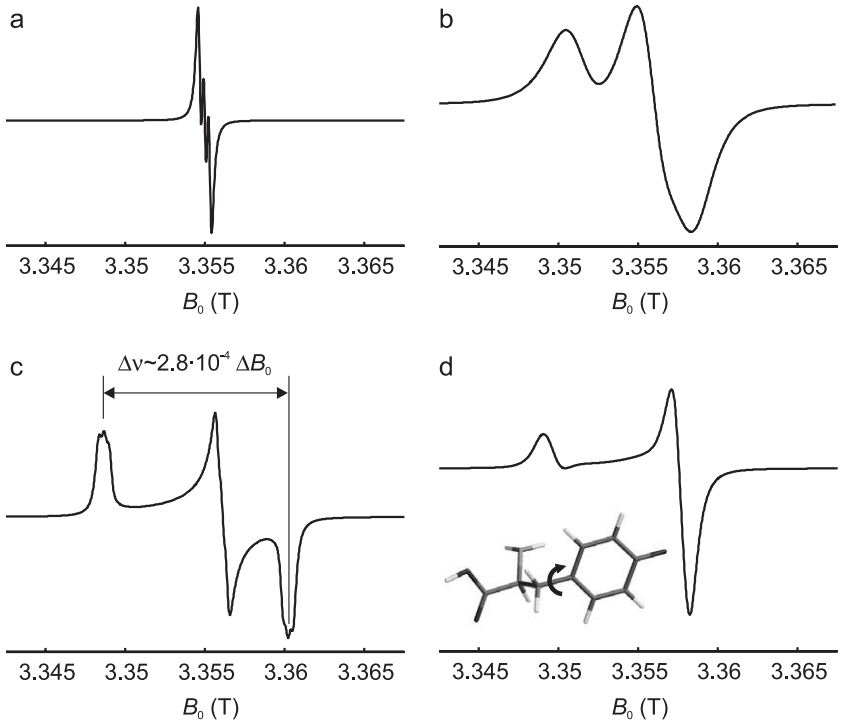

Fig. 2. Influence of rotational diffusion on the W-band EPR spectrum of a perdeuterated tyrosyl radical (simulations using the software package described in Ref. [75], $g_x = 2.0091$, $g_y = 2.0046$, $g_z = 2.0021$, $A_{\beta 1} = 0.3$ mT). (a) Fast limit, $\tau_c = 10$ ps. (b) Slow tumbling, $\tau_c = 1/\Delta\nu = 3$ ns. (c) Rigid limit, $\tau_c = 1$ μs. (d) Anisotropic rotational diffusion with a rotational diffusion tensor of axial symmetry, rotation about the axis parallel to the C—O· bond with $\tau_c = 0.3$ ns, rotation about the other axes with $\tau_c = 30$ ns.

To the best of our knowledge, reorientation dynamics of native radical species in enzymes has not yet been characterised by EPR spectroscopy. To some extent, this is because radicals in electron transfer chains are too short-lived to be studied at room temperature. However, spectra can be acquired at room temperature in several cases, for instance for tyrosyl radicals in Photosystem II [78] and tryptophanyl radicals in ribonucleotide reductase [79]. Since rotational correlation times of soluble proteins at room temperature are of the order of 10 ns these spectra are likely to correspond to the slow tumbling regime if the hyperfine anisotropy is of the order of 10 MHz or if the measurements are performed at high fields. A rotational correlation time of approximately 2 ns was recently found by fluorescence techniques for a bound flavin cofactor in flavocytochrome(*b*2) at room temperature [80]. As shown in Fig. 2, correlation times like this correspond to the slow tumbling regime in high-field EPR.

4. The biochemist's view: getting information on protein function

4.1. Identification of radical species

Enzymes that catalyse processes involving a one-electron reduction or oxidation step are candidates for the occurrence of transient radicals. Detection of such radicals is sometimes possible by just adding the substrate to the enzyme and measuring the EPR spectrum at room temperature. In other cases, measurements must be performed at low temperatures to obtain sufficient sensitivity or resolution. To check whether the observed radical is in fact the initially formed and kinetically competent radical or the product of a side reaction, it may be necessary to perform freeze-quench experiments at a time scale of a few seconds [1].

Once it is ascertained that the observed radical is of interest for enzyme function, its structure has to be identified. The classical way for this is observing EPR spectral changes caused by isotope substitution. By comparing spectra of the B2 subunit of ribonucleotide reductase from *E. coli* bacteria grown in H_2O and D_2O medium, the hyperfine splitting of approximately 1.6 mT could be traced back to a proton [81]. Using D_2O growth media with different combinations of deuterated and non-deuterated amino acids, the radical could be attributed to a tyrosine residue **1**. The glycyl radical **2** in pyruvate formate-lyase was identified by a similar procedure [82]. However, in this case ^{13}C substitution instead of deuteration was found to be necessary as the α hydrogen of the glycyl radical proved to be solvent-exchangeable.

The advent of high-field/high-frequency EPR has made it possible to identify known radicals by their *g* tensor principal values (Table 1). For previously unknown radicals or in ambiguous situations, isotope substitution may, however, still be the most reliable procedure. Increasingly, DFT

computations can help in identification and in assigning lines in the spectra.

If the EPR spectrum is much too broadened or untypical, which may be caused by coupling to a nearby metal centre, both approaches discussed above may fail. This problem was solved in the identification of the tryptophanyl radical in cytochrome *c* peroxidase by resorting to ENDOR experiments on isotopically substituted samples [83]. In this case, weak exchange coupling to the oxyferryl heme suffices to spoil EPR resolution but does not significantly influence the apparent hyperfine couplings observed in the ENDOR experiments. As an additional benefit of a full analysis of the hyperfine structure, it could be shown that the species is a π cation radical rather than a neutral tryptophanyl radical.

Another instance of a featureless EPR line is the tryptophanyl tryptophyl-semiquinone intermediate of methylamine dehydrogenase [34]. Here, ESEEM spectroscopy was applied to measure ^{14}N hyperfine and nuclear quadrupole couplings and isotope substitution of ^{14}N by ^{15}N in the substrate served to prove that the semiquinone exist in the N-form with a substrate-derived imine-nitrogen.

4.2. Separation of several species

For some radical enzymes, it has been suggested that their mechanism involves the transfer of the unpaired electron via several residues over distances of some 10 Å [1]. Freeze-quenched samples may then contain several radical species whose EPR spectra overlap. A case in point are observations on the E441Q mutant of the R1 subunit of the *E. coli* class I ribonucleotide reductase [84]. At a temperature of 20 K, the high-frequency (140 GHz) stimulated echo-detected EPR spectrum of a freeze-quenched reaction mixture with cystidine 5′-diphosphate exhibits a superposition of at least two spectral components, one of which could be assigned to a tyrosyl radical **1** based on its *g* tensor principal values. Increasing the temperature to 60 K results in suppression of the tyrosyl contribution due to fast relaxation of the electron spins induced by the nearby diferric cluster. This suppression of fast-relaxing components is a feature of the stimulated echo sequence used for detection. The spectrum at 60 K still consists of two components which could be separated by their kinetics by measuring samples quenched at different waiting times after preparing the reaction mixture. One of the components was identified as a disulfide radical which is probably involved in the normal reaction pathway of this enzyme, while the second component may be a ketyl radical that is not on this pathway. Relaxation contrast as used in this example might also become a valuable tool for separating contributions of organic radicals from those of paramagnetic metal centres.

4.3. Radical quantification and reaction kinetics

Understanding mechanism and function of radical enzymes requires some information on radical concentration and lifetime. Absolute measurements of radical concentrations are usually performed by comparing the double integral of the CW EPR spectrum of the enzyme radical to the double integral of the spectrum an external standard, such as a nitroxide radical [85]. The external standard should be dissolved in a solvent that mimics as closely as possible the dielectric properties of the enzyme sample. Furthermore, measurement conditions, including positioning of the sample in the resonator, have to be exactly the same for both samples. Saturation must be avoided for either of the two samples. Adjustment of the phase and baseline correction before integration are critical. Even if all these precautions are taken, absolute concentrations determined by EPR spectroscopy with external standards may deviate from true values by up to $\sim 30\%$, a fact that is sometimes not appreciated.

Measurements of relative concentrations in a series of spectra with the same line shape do not require double integration, but can rather be done by comparing signal amplitudes. This eliminates baseline uncertainty as a major error source, so that data points in a kinetic trace can be determined with a precision of $\sim 5\%$.

Based on such measurements, it is possible to compare the kinetics of formation and decay of EPR-detectable radicals to the kinetics of metabolite formation and decay. For instance, a semiquantitative kinetic analysis of EPR-detectable tyrosyl radicals **1** in prostaglandin H synthase on a minute time scale by a freeze-quench technique revealed that these radicals are not catalytically competent intermediates in the cyclooxygenase activity of this enzyme [85]. Furthermore, this study indicated that, for the enzyme reconstituted with Fe(III)-protoporphyrin IX, the radicals are in some way related to peroxidase activity. In a study on DNA photolyase, kinetics could be observed on a much shorter time scale by time-resolved EPR techniques, since in this case the reaction can be initiated by a light flash [86]. The observations suggests that the characteristic decay time of the photoinitiated tryptophan radicals is not much longer than the duration of the applied light flash (17 μs).

4.4. Localisation of radicals

Identification of the structure of the radical is usually insufficient for determining where exactly in the protein the radical is generated. In the case of glycine radicals, this question can be solved by fragmenting the peptide chain at the radical site with oxygen and determining the terminal sequences of the resulting fragments [82]. Another non-EPR technique for identifying the residue that corresponds to an amino acid radical is site-directed mutagenesis. It should be noted, however, that mutation of residues close to the catalytical centre may cause self-destruction of the enzyme whether or not the residue is directly involved in the electron transfer [1].

As primary radicals in enzymes are usually generated by electron transfer from a metal centre, they are likely to be

close to such a centre. Such proximity between the tyrosyl radical and the dinuclear iron cluster cofactor was proved for ribonucleotide reductase of *E. coli* by iron isotope substitution (^{57}Fe), which led to broadening of the signal [87]. A more quantitative characterisation of this interaction was achieved by analysing the enhancement of longitudinal relaxation of the tyrosyl radical by the iron cluster [65]. An interaction between a thiyl radical and the Cob(II)alamin cofactor in ribonucleoside triphosphate reductase from *Lactobacillus leichmannii* was indicated by observing changes in the EPR spectrum on substituting cysteine by (β-^{2}H-cysteine) and by successful simulation of the EPR spectra measured at X-band and Q-band with the same parameters set for a two-spin model, whereas a single-spin model could not fit the spectra [88].

A hitherto unused possibility of localising radicals in a protein derives from site-directed spin labeling techniques, in which selected residues are mutated to cysteins and a thiol-specific nitroxide spin label is attached to them [89]. Distances up to 20 Å between two such labels can be estimated from CW EPR spectra with small amounts (50–100 pmol) of doubly spin-labeled protein. The same method should be applicable to estimating the distance between a native radical in an enzyme and one nitroxide label at a known residue. Precise measurements of such spin-to-spin distances between 20 and at least 50 Å and the characterisation of distance distributions are possible with pulse EPR methods [66,72]. Our own recent experiments indicate that at least 5–10 nmol protein are required in this case. Accessing such large distances would allow to use nitroxide spin labels at residues that are sufficiently far removed from the active centre, so that function is not influenced. Using triangulation techniques [90], it may then be possible to localise the radical with a precision of approximately 1–2 Å.

Such precision may still be insufficient for discussing certain aspects of the structure–function relationship. A case in point is the displacement of the tyrosyl radical cofactor in ribonucleotide reductase in the active state compared to the resting state [91]. By high-frequency (94 GHz) EPR on a single crystal it was possible to derive the orientation of the *g* tensor principal axes and thus of the molecular frame with respect to the crystal frame. Compared to the X-ray crystal structure of the resting state, the tyrosyl side chain is rotated by approximately 10° away from the diiron centre, which probably corresponds to the breaking of a weak hydrogen bond to the diiron site. This conformational change may be connected to the stabilisation of the radical. It should be noted, however, that conformational changes in protein crystals are likely to be smaller than in vivo. This is because packing effects in the crystal may restrict the freedom of flexible parts of the protein, as was found by comparison of NMR and X-ray structures (for a recent example, see Ref. [92]). By comparing structures of proteins that have been crystallised in different unit cells, it was found that amino acid side-chain conformations are quite often influenced by such packing effects [93].

In the case of pyruvate formate-lyase activating enzyme a precursor of an adenosyl radical could be precisely localised by an Q-band ENDOR study on the $[4Fe–4S]^+$ cluster in the presence of *S*-adenosylmethionine (AdoMet) [94]. Addition of AdoMet to the photoreduced enzyme results in a change of the *g* tensor of the iron–sulfur cluster from rhombic to nearly axial symmetry. Field-dependent ^{2}H ENDOR (orientation selection) using CD_3-AdoMet and ^{13}C ENDOR using $^{13}CH_3$-AdoMet provided estimates for the distance of the methyl group of AdoMet from the iron cluster, which in turn suggested a structural model for the coordination and a proposal for the mechanism of formation of the adenosyl radical.

4.5. Control of the reaction mechanism by the radical environment

Radical enzymes are studied with the ultimate goal to understand how these natural systems catalyse chemical reactions with high specificity and under mild conditions. This is a complex problem which involves, among others, questions about control of the spatial arrangement of educts and catalytic centre, about fine-tuning of chemical potentials, and about stabilisation of reactive intermediates. In the context of radical enzymes, these questions are closely related to differences in electronic structure and in mobility between a freely diffusing radical with low molecular mass on the one hand and a protein-bound or protein-embedded radical on the other hand. To date, the mechanism of none of the known radical enzymes appears to be understood in such detail.

On the other hand, many tools for addressing the underlying questions by EPR spectroscopy have been developed in the past few years and continue to be developed. The sensitivity of the *g* tensor and of hyperfine tensors to polarity of the environment and formation of hydrogen bonds will allow for comparison of electronic structures in different environments once a sufficiently large database is established. For instance, protein-bound or -embedded semiquinone radicals appear to be stabilised by hydrogen-bonding whose details differ between different proteins. A recent multi-frequency EPR study of ubiquinol oxidase bo_3 from *E. coli* with ubiquinone selectively ^{13}C-labeled at either the 1- or 4-carbonyl carbon demonstrates that the spin density distribution is strongly asymmetric in this case, which may be related to the direction of electron transfer via this semiquinone [48]. DFT computations should be helpful for understanding such differences and to relate them to changes in chemical potential or, in the case at hand, to the proposed ‘‘diode’’ function of the quinone in electron transfer.

Insight into control of the reaction mechanism can also be expected from the characterisation of the geometry of intermediates by ENDOR or ESEEM spectroscopy and from monitoring conformational changes between the resting state and the active state in protein crystals by high-field

EPR or by combining site-directed spin labeling and EPR distance measurements. The latter approach, which has been fairly successful for other proteins [89], has the advantage that it does not rely on protein crystals and may thus more closely mimic the situation in vivo.

Finally, control of radical reactions in proteins is very likely related to the restricted mobility of the radical. By kinetic control, this restriction can prevent side reactions which would be thermodynamically feasible. Concepts of polymer dynamics and experimental data on protein dynamics gathered by site-directed spin-labeling studies or by NMR techniques could guide such work. It remains an experimental challenge, however, to obtain high-field CW EPR spectra of radicals in proteins with a sufficient signal-to-noise ratio for line shape analysis.

5. Conclusion

EPR spectroscopy is the main technique for identifying radicals in enzymes. Beyond that, advances in high-frequency and multi-frequency EPR spectroscopy, in DFT computations of hyperfine couplings and *g* tensors, and in the application of ENDOR and ESEEM techniques to proteins increasingly provide insight into interactions of these radicals with the protein and with other cofactors. Characterising and understanding global and local conformational changes in the enzyme and their relation to reaction control may be one of the challenges for future EPR studies in this field. The parallel development during the past few years of site-directed spin-labeling and of EPR techniques for distance measurements may have created the tools for meeting this challenge.

Acknowledgements

The author thanks an anonymous referee for helpful suggestions. Financial help by a Dozentenstipendium of Fonds der Chemischen Industrie is gratefully acknowledged.

References

[1] J. Stubbe, W.A. van der Donk, Protein radicals in enzyme catalysis, Chem. Rev. 98 (1998) 705–762.
[2] P.A. Frey, Radical mechanisms of enzymatic catalysis, Ann. Rev. Biochem. 70 (2001) 121–148.
[3] J.Z. Pedersen, A. Finazzi-Agrò, Protein-radical enzymes, FEBS Lett. 325 (1993) 53–58.
[4] M. Fontecave, Ribonucleotide reductases and radical reactions, Cell. Mol. Life Sci. 54 (1998) 684–695.
[5] G. Sawers, Biochemistry, physiology and molecular biology of glycyl radical enzymes, FEMS Microbiol. Rev. 22 (1999) 543–551.
[6] A.J. Hoff (Ed.), Advanced EPR, Elsevier, Amsterdam, 1989.
[7] A. Schweiger, G. Jeschke, Principles of Pulse Electron Paramagnetic Resonance, Oxford Univ. Press, Oxford, 2001.
[8] S. Un, P. Dorlet, A.W. Rutherford, A high-field EPR tour of radicals in photosystems I and II, Appl. Magn. Reson. 21 (2001) 341–361.
[9] K.K. Andersson, P.P. Schmidt, B. Katterle, K.R. Strand, A.E. Palmer, S.K. Lee, E.I. Solomon, A. Gräslund, A.L. Barra, Examples of high-frequency EPR studies in bioinorganic chemistry, J. Biol. Inorg. Chem. 8 (2003) 235–247.
[10] K. Möbius, Primary processes in photosynthesis: what do we learn from high-field EPR spectroscopy? Chem. Soc. Rev. 29 (2000) 129–139.
[11] W. Lubitz, F. Lendzian, R. Bittl, Radicals, radical pairs and triplet states in photosynthesis, Acc. Chem. Rev. 35 (2002) 313–320.
[12] F. Rappaport, J. Lavergne, BBA Bioenerg. 1503 (2001) 246–259.
[13] R.P. Pesavento, W.A. Van Der Donk, Tyrosyl radical cofactors, Adv. Protein Chem. 58 (2001) 317–385.
[14] G.J. Gerfen, B.F. Bellew, S. Un, J.M. Bollinger, J.A. Stubbe, R.G. Griffin, D.J. Singel, High-frequency (139.5 GHz) EPR spectroscopy of the tyrosyl radical in *Escherichia coli* ribonucleotide reductase, J. Am. Chem. Soc. 115 (1993) 6420–6421.
[15] A. Ivancich, P. Dorlet, D.B. Goodin, S. Un, Multifrequency high-field EPR study of the tryptophanyl and tyrosyl radical intermediates in wild-type and the W191G mutant of cytochrome *c* peroxidase, J. Am. Chem. Soc. 123 (2001) 5050–5058.
[16] S. Un, C. Gerez, E. Elleingand, M. Fontecave, Sensitivity of tyrosyl radical *g*-values to changes in protein structure: a high-field EPR study of mutants of ribonucleotide reductase, J. Am. Chem. Soc. 123 (2001) 3048–3054.
[17] K.K. Andersson, A.L. Barra, The use of high field/frequency EPR in studies of radical and metal sites in proteins and small inorganic models, Spectrochim. Acta, A Mol. Spectrosc. 58 (2002) 1101–1112.
[18] M. Bennati, C.T. Farrar, J.A. Bryant, S.J. Inati, V. Weis, G.J. Gerfen, P. Riggs-Gelasco, J. Stubbe, R.G. Griffin, Pulsed electron-nuclear double resonance (ENDOR) at 140 GHz, J. Magn. Reson. 138 (1999) 232–243.
[19] G. Bleifuss, M. Kolberg, S. Pötsch, W. Hofbauer, R. Bittl, W. Lubitz, A. Gräslund, G. Lassmann, F. Lendzian, Tryptophan and tyrosine radicals in ribonucleotide reductase: a comparative high-field EPR study at 94 GHz, Biochemistry 40 (2001) 15362–15368.
[20] C. Aubert, M.H. Vos, P. Mathis, A.P.M. Eker, K. Brettel, Intraprotein radical transfer during photoactivation of DNA photolyase, Nature 405 (2000) 586–590.
[21] L. Eberson, Spin trapping and electron transfer, Adv. Phys. Org. Chem. 31 (1998) 91–141.
[22] W. Blodig, A.T. Smith, K. Winterhalter, K. Piontek, Evidence from spin-trapping for a transient radical on tryptophan residue 171 of lignin peroxidase, Arch. Biochem. Biophys. 370 (1999) 86–92.
[23] E. Mulliez, M. Fontecave, J. Gaillard, P. Reichard, An iron–sulfur center and a free radical in the active anaerobic ribonucleotide reductase of *Escherichia coli*, J. Biol. Chem. 268 (1993) 2296–2299.
[24] C. Duboc-Toia, A.K. Hassan, E. Mulliez, S. Ollagnier-de Choudens, M. Fontecave, C. Leutwein, J. Heider, Very high-field EPR study of glycyl radical enzymes, J. Am. Chem. Soc. 125 (2003) 38–39.
[25] A. Becker, W. Kabsch, X-ray structure of pyruvate formate-lyase in complex with pyruvate and CoA—how the enzyme uses the Cys-418 thiyl radical for pyruvate, J. Biol. Chem. 277 (2002) 40036–40042.
[26] D. Nelson, M.C.R. Symons, The detection of thiyl radicals by ESR spectroscopy, Chem. Phys. Lett. 36 (1975) 340–341.
[27] Y.R. Chen, M.R. Gunther, R.P. Mason, An electron spin resonance spin-trapping investigation of the free radicals formed by the reaction of mitochondrial cytochrome *c* oxidase with H_2O_2, J. Biol. Chem. 274 (1999) 3308–3314.
[28] M. Kolberg, G. Bleifuss, A. Gräslund, B.-M. Sjöberg, W. Lubitz, F. Lendzian, G. Lassmann, Generation and electron paramagnetic resonance spin trapping detection of thiyl radicals in model proteins and in the R1 subunit of *Escherichia coli* ribonucleotide reductase, Arch. Biochem. Biophys. 397 (2002) 57–68.
[29] M. Kolberg, G. Bleifuss, A. Gräslund, B.-M. Sjöberg, W. Lubitz, F.

Lendzian, G. Lassmann, Protein thiyl radicals directly observed by EPR spectroscopy, Arch. Biochem. Biophys. 403 (2002) 141–144.
[30] F. Lendzian, Amino acid radicals in ribonucleotide reductase studied by high-field EPR and ENDOR, Biochim. Biophys. Acta, this issue.
[31] R. Medda, A. Padiglia, A. Bellelli, J.Z. Pedersen, A. Finazzi-Agrò, G. Floris, CuI-semiquinone radical species in plant copper-amine oxidases, FEBS Lett. 453 (1999) 1–5.
[32] J. McCracken, J. Peisach, C.E. Cote, M.A. McGuirl, D.M. Dooley, Pulsed EPR studies of the semiquinone state of copper-containing amine oxidases, J. Am. Chem. Soc. 114 (1992) 3715–3720.
[33] S. de Vries, R.J.M. van Spanning, V. Steinebach, A spectroscopic and kinetic study of *Escherichia coli* amine oxidase, J. Mol. Catal. 8 (2000) 111–120.
[34] V. Singh, Z. Zhu, V.L. Davidson, J. McCracken, Characterization of the tryptophan tryptophyl-semiquinone catalytic intermediate of methylamine dehydrogenase by electron spin-echo envelope modulation spectroscopy, J. Am. Chem. Soc. 122 (2000) 931–938.
[35] J.W. Whittaker, Galactose oxidase, Adv. Protein Chem. 60 (2002) 1–49.
[36] S.J. Firbank, M.S. Rogers, C.M. Wilmot, D.M. Dooley, M.A. Halcrow, P.F. Knowles, M.J. McPherson, S.E.V. Phillips, Crystal structure of the precursor of galactose oxidase: an unusual self-processing enzyme, Proc. Natl. Acad. Sci. U. S. A. 98 (2001) 12932–12937.
[37] M.M. Whittaker, J.W. Whittaker, Cu(I)-dependent biogenesis of the galactose oxidase redox cofactor, J. Biol. Chem. 278 (2003) 22090–22101.
[38] J.W. Whittaker, Free radical catalysis by galactose oxidase, Chem. Rev. 103 (2003) 2347–2363.
[39] G.J. Gerfen, B.F. Bellew, R.G. Griffin, D.J. Singel, C.A. Ekberg, J.W. Whittaker, High-frequency electron paramagnetic resonance spectroscopy of the apogalactose oxidase radical, J. Phys. Chem. 100 (1996) 16739–16748.
[40] M. Kaupp, T. Gress, R. Reviakine, O.L. Malkina, V.G. Malkin, *g* Tensor and spin density of the modified tyrosyl radical in galactose oxidase: a density functional study, J. Phys. Chem., B 107 (2003) 331–337.
[41] S.X. Wang, M. Mure, K.F. Medzihradszky, A.L. Burlingame, D.E. Brown, D.M. Dooley, A.J. Smith, H.M. Kagan, J.P. Klinman, A crosslinked cofactor in lysyl oxidase: redox function for amino acid side chains, Science 273 (1996) 1078–1084.
[42] A.P. Bussandri, C.W. Kiarie, H. Van Willigen, Photoinduced bond homolysis of B-12 coenzymes. An FT-EPR study, Res. Chem. Intermed. 28 (2002) 697–710.
[43] L. Kerscher, D. Oesterhelt, The catalytic mechanism of 2-oxoacid-ferredoxin oxidoreductases from halobacterium-halobium-one-electron transfer at 2 distinct steps of the catalytic cycle, Eur. J. Biochem. 116 (1981) 595–600.
[44] V.F. Bouchev, C.M. Furdui, S. Menon, R.B. Muthukumaran, S.W. Ragsdale, J. McCracken, ENDOR studies of pyruvate: ferredoxin oxidoreductase reaction intermediates, J. Am. Chem. Soc. 121 (1999) 3724–3729.
[45] E. Chabriere, C. Vernede, B. Guigliarelli, M.H. Charon, E.C. Hatchikian, cilla-Camps, J.C. Fontecilla-Camps, Crystal structure of the free radical intermediate of pyruvate: ferredoxin oxidoreductase, Science 294 (2001) 2559–2563.
[46] B.L. Trumpower (Ed.), Function of Quinones in Energy Conserving Systems, Academic Press, New York, 1982.
[47] J.A. Pedersen, EPR Spectra from Natural and Synthetic Quinones and Quinoids, CRC Press, Boca Raton, 1985.
[48] S. Grimaldi, T. Ostermann, N. Weiden, T. Mogi, H. Miyoshi, B. Ludwig, H. Michel, T.F. Prisner, F. MacMillan, Asymmetric binding of the high-affinity QH^- ubisemiquinone in quinol oxidase (bo_3) from *Escherichia coli* studied by multifrequency electron paramagnetic resonance spectroscopy, Biochemistry 42 (2003) 5632–5639.
[49] B.J. Hales, Immobilized radicals: 2. Hydrogen-bonding of the semiquinone anion radical, J. Am. Chem. Soc. 98 (1976) 7350–7357.
[50] O. Burghaus, M. Plato, M. Rohrer, K. Möbius, F. MacMillan, W. Lubitz, 3-mm high-field EPR EPR on semiquinone radical anions $Q^{\cdot -}$ related to photosynthesis and on the primary donor $P^{\cdot +}$ and acceptor $QA^{\cdot -}$ in reaction centers of *Rhodobacter sphaeroides* R-26, J. Phys. Chem. 97 (1993) 7639–7647.
[51] M. Knüpling, J.T. Törring, S. Un, The relationship between the molecular structure of semiquinone radicals and their *g*-values, Chem. Phys. 219 (1997) 291–304.
[52] M. Kaupp, C. Remenyi, J. Vaara, O.L. Malkina, V.G. Malkin, Density functional calculations of electronic *g*-tensors for semiquinone radical anions. The role of hydrogen bonding and substituent effects, J. Am. Chem. Soc. 124 (2002) 2709–2722.
[53] B. Barquera, J.E. Morgan, D. Lukoyanov, C.P. Scholes, R.B. Gennis, M.J. Nilges, X- and W-band EPR and Q-band ENDOR studies of the flavin radical in the Na^+-translocating NADH:quinone oxidoreductase from *Vibrio cholerae*, J. Am. Chem. Soc. 125 (2003) 265–275.
[54] M.R. Fuchs, E. Schleicher, A. Schnegg, C.W.M. Kay, J.T. Torring, R. Bittl, A. Bacher, G. Richter, K. Mobius, S. Weber, *g*-Tensor of the neutral flavin radical cofactor of DNA photolyase revealed by 360-GHz electron paramagnetic resonance spectroscopy, J. Phys. Chem., B 106 (2002) 8885–8890.
[55] A.J. Stone, *g*-Factors of aromatic free radicals, Mol. Phys. 6 (1963) 509–515.
[56] T. Kawamura, S. Matsunami, T. Yonezawa, Solvent effects on the *g*-value of di-*t*-butyl nitric oxide, Bull. Chem. Soc. Jpn. 40 (1967) 1111–1115.
[57] M.H. Lim, S.E. Worthington, F.J. Dulles, C.J. Cramer, Density-functional calculations of radicals and diradicals, ACS Symp. Ser. 629 (1996) 402–422.
[58] F.Q. Ban, K.N. Rankin, J.W. Gauld, R.J. Boyd, Recent applications of density functional theory calculations to biomolecules, Theor. Chem. Acc. 108 (2002) 1–11.
[59] H.J. Steinhoff, A. Savitsky, C. Wegener, M. Pfeiffer, M. Plato, K. Möbius, High-field EPR studies of the structure and conformational changes of site-directed spin labeled bacteriorhodopsin, Biochim. Biophys. Acta 1457 (2000) 253–262.
[60] H. Kurreck, B. Kirste, W. Lubitz, Electron Nuclear Double Resonance Spectroscopy of Radicals in Solution, VCH, New York, 1988.
[61] W.B. Mims, J. Peisach, in: L. Berliner, J. Reuben (Eds.), Biological Magnetic Resonance, vol. 3, Plenum, New York, 1981, Chap. 5, pp. 213–263.
[62] Y. Deligiannakis, A. Ivancich, A.W. Rutherord, 2D-hyperfine sublevel correlation spectroscopy of tyrosyl radicals, Spectrochim. Acta, A Mol. Spectrosc. 58 (2002) 1191–1200.
[63] D. Goldfarb, V. Kofman, J. Libman, A. Shanzer, R. Rahmatouline, S. Van Doorslaer, A. Schweiger, Double nuclear coherence transfer (DONUT)-HYSCORE: a new tool for the assignment of nuclear frequencies in pulsed EPR experiments, J. Am. Chem. Soc. 120 (1998) 7020–7029.
[64] A. Fournel, S. Gambarelli, B. Guigliarelli, C. More, M. Asso, G. Chouteau, R. Hille, P. Bertrand, Magnetic interactions between a [4Fe–4S](1+) cluster and a flavin mononucleotide radical in the enzyme trimethylamine dehydrogenase: a high-field electron paramagnetic resonance study, J. Chem. Phys. 109 (1998) 10905–10913.
[65] C. Galli, M. Atta, K.K. Andersson, A. Gräslund, G.W. Brudvig, Variations of the diferric exchange coupling in the R2 subunit of ribonucleotide reductase from four species as determined by saturation-recovery EPR spectroscopy, J. Am. Chem. Soc. 117 (1995) 740–746.
[66] L.J. Berliner, S.S. Eaton, G.R. Eaton (Eds.), Biological Magnetic Resonance, vol. 19, Kluwer Academic Publishing, Amsterdam, 2001.
[67] R. Calvo, E.C. Abresch, R. Bittl, G. Feher, W. Hofbauer, R.A. Isaacson, W. Lubitz, M.Y. Okamura, M.L. Paddock, EPR study of the molecular and electronic structure of the semiquinone biradical $QA^{-}\cdot QB^{-\cdot}$ in photosynthetic reaction centers from *Rhodobacter sphaeroides*, J. Am. Chem. Soc. 122 (2000) 7327–7341.
[68] C. Elsasser, M. Brecht, R. Bittl, Pulsed electron–electron double

resonance on multinuclear metal clusters: assignment of spin projection factors based on the dipolar interaction, J. Am. Chem. Soc. 124 (2002) 12606–12611.
[69] A. Schweiger, Pulsed electron-spin-resonance spectroscopy—basic principles, techniques, and examples of applications, Angew. Chem., Int. Ed. Engl. 30 (1991) 265–292.
[70] A.V. Astashkin, A.M. Raitsimring, F.A. Walker, Two- and four-pulse ESEEM studies of the heme binding center of a low-spin ferriheme protein: the importance of a multi-frequency approach, Chem. Phys. Lett. 306 (1999) 9–17.
[71] T. Ichikawa, L. Kevan, M.K. Bowman, S.A. Dikanov, Yu.D. Tsvetkov, Ratio analysis of electron-spin echo modulation envelopes in disordered matrices and application to the structure of solvated electrons in 2-methyltetrahydrofuran glass, J. Chem. Phys. 71 (1979) 1167–1174.
[72] G. Jeschke, Distance measurements in the nanometer range by pulse EPR, Chem. Phys. Chem. 3 (2002) 927–932.
[73] D. Marsh, V.A. Livshits, T. Pali, Non-linear, continuous-wave EPR spectroscopy and spin-lattice relaxation: spin-label EPR methods for structure and dynamics, J. Chem. Soc., Perkin Trans. 2 (1997) 2545–2548.
[74] J.H. Freed, in: L.J. Berliner (Ed.), Spin Labeling: Theory and Applications, Academic Press, New York, 1976, pp. 53–132.
[75] D.J. Schneider, J.H. Freed, Calculating Slow Motional Magnetic Resonance Spectra: A User's Guide, in: L.J. Berliner, J. Reuben (Eds.), Biological Magnetic Resonance, vol. 8, Plenum, New York, 1989, pp. 1–75.
[76] D. Kivelson, Theory of linewidths of free radicals, J. Chem. Phys. 33 (1960) 1094–1106.
[77] H.J. Steinhoff, W.L. Hubbell, Calculation of electron paramagnetic resonance spectra from Brownian dynamics trajectories: application to nitroxide side chains in proteins, Biophys. J. 71 (1996) 2201–2212.
[78] R.J. Boerner, B.A. Barry, Isotopic labeling and EPR spectroscopy show that a tyrosine residue is the terminal electron-donor, Z, in manganese-depleted photosystem-II preparations, J. Biol. Chem. 268 (1993) 17151–17154.
[79] M. Sahlin, G. Lassmann, S. Potsch, A. Slaby, B.M. Sjoberg, A. Graslund, Tryptophan radicals formed by iron/oxygen reaction with *Escherichia coli* ribonucleotide reductase protein R2 mutant Y122F, J. Biol. Chem. 269 (1994) 11699–11702.
[80] J.R. Albani, A. Sillen, Y. Engelborghs, M. Gervais, Dynamics of flavin in flavocytochrome *b*(2): a fluorescence study, Photochem. Photobiol. 69 (1999) 22–26.
[81] B.-M. Sjöberg, P. Reichard, A. Gräslund, A. Ehrenberg, Nature of the free radical in ribonucleotide reductase from *Escherichia coli*, J. Biol. Chem. 252 (1977) 536–541.
[82] A.F.V. Wagner, M. Frey, F.A. Neugebauer, W. Schäfer, J. Knappe, The free radical in pyruvate formate-lyase is located on glycine-734, Proc. Natl. Acad. Sci. U. S. A. 89 (1992) 996–1000.
[83] J.E. Huyett, P.E. Doan, R. Gurbiel, A.L.P. Houseman, M. Sivaraja, D.B. Goodin, B.M. Hoffman, Compound ES of cytochrome *c* peroxidase contains a Trp π-cation radical: characterization by CW and pulsed Q-band ENDOR spectroscopy, J. Am. Chem. Soc. 117 (1995) 9033–9041.
[84] C.C. Lawrence, M. Bennati, H.V. Obias, G. Bar, R.G. Griffin, J. Stubbe, High-field EPR detection of a disulfide radical anion in the reduction of cytidine 5′-diphosphate by the E441Q R1 mutant of *Escherichia coli* ribonucleotide reductase, Proc. Natl. Acad. Sci. U. S. A. 96 (1999) 8979–8984.
[85] G. Lassmann, R. Odenwaller, J.F. Curtis, J.A. DeGray, R.P. Mason, L.J. Marnett, T.E. Eling, Electron spin resonance investigation of tyrosyl radicals of prostaglandin H synthase, J. Biol. Chem. 266 (1991) 20045–20055.
[86] S.T. Kim, A. Sancar, C. Essenmacher, G.T. Babcock, Time-resolved EPR studies with DNA photolyase-excited-state FADH(0) abstracts an electron from Trp-306 to generate $FADH^-$, the catalytically active form of the cofactor, Proc. Natl. Acad. Sci. U. S. A. 90 (1993) 8023–8027.
[87] J.M. Bollinger, D.E. Edmondson, B.H. Huynh, J. Filley, J.R. Norton, J. Stubbe, Mechanism of assembly of the tyrosyl radical-dinuclear iron cluster cofactor of ribonucleotide reductase, Science 253 (1991) 292–298.
[88] G.J. Gerfen, S. Licht, J.P. Willems, B.M. Hoffman, J. Stubbe, Electron paramagnetic resonance investigations of a kinetically competent intermediate formed in ribonucleotide reduction: evidence for a thiyl radical-Cob(II)alamin interaction, J. Am. Chem. Soc. 118 (1996) 8192–8197.
[89] W.L. Hubbell, D.S. Cafioso, C. Altenbach, Identifying conformational changes with site-directed spin labeling, Nat. Struct. Biol. 7 (2000) 735–739.
[90] P.P. Borbat, H.S. Mchaourab, J.H. Freed, Protein structure determination using long-distance constraints from double-quantum coherence ESR: study of T4 lysozyme, J. Am. Chem. Soc. 124 (2002) 5304–5314.
[91] M. Hogbom, M. Galander, M. Andersson, M. Kolberg, W. Hofbauer, G. Lassmann, P. Nordlung, F. Lendzian, Displacement of the tyrosyl radical cofactor in ribonucleotide reductase obtained by single-crystal high-field EPR and 1.4-Angstrom X-ray data, Proc. Natl. Acad. Sci. U. S. A. 100 (2003) 3209–3214.
[92] M.L. Raves, J.F. Doreleijers, H. Vis, C.E. Vorgias, K.S. Wilson, R. Kaptein, Joint refinement as a tool for thorough comparison between NMR and X-ray data and structures of HU protein, J. Biomol. NMR 21 (2001) 235–248.
[93] M.P. Jacobson, R.A. Friesner, Z.X. Xiang, B. Honig, On the role of the crystal environment in determining protein side-chain conformations, J. Mol. Biol. 320 (2002) 597–608.
[94] C.J. Walsby, W. Hong, W.E. Broderick, J. Cheek, D. Ortillo, J.B. Broderick, B.M. Hoffman, Electron-nuclear double resonance spectroscopic evidence that *S*-adenosylmethionine binds in contact with the catalytically active [4Fe–4S]+ cluster of pyruvate formate-lyase activating enzyme, J. Am. Chem. Soc. 124 (2002) 3143–3151.